Journal of ELECTRONIC MATERIALS, Vol. 39, No. 12, 2010
DOI: 10.1007/s11664-010-1372-4

Effects of Minor Ni Doping on Microstructural Variations and Interfacial Reactions in Cu/Sn-3.0Ag-0.5Cu-*x*Ni/Au/Ni Sandwich Structures

CHI-YANG YU,[1] TAE-KYU LEE,[2] MICHAEL TSAI,[2] KUO-CHUAN LIU,[2] and JENQ-GONG DUH[1,3]

1.—Department of Materials Science and Engineering, National Tsing Hua University, Hsinchu, Taiwan. 2.—Interconnect Technology Team, Manufacturing Technology Group, Cisco Systems, Inc., San Jose, CA, USA. 3.—e-mail: jgd@mx.nthu.edu.tw

The effects of Ni doping on microstructural variations and interfacial reactions in Cu/Sn-3.0Ag-0.5Cu-*x*Ni/Au/Ni sandwich structures were investigated. The sandwich structures, i.e., Cu/Sn-3.0Ag-0.5Cu/Au/Ni and Cu/Sn-3.0Ag-0.5Cu-0.1Ni/Au/Ni (wt.%), were reflowed and isothermally aged at 150°C for 500 h. The behavior of Ni and Cu migration in the solders before and after aging was investigated using field-emission electron probe microanalysis (FE-EPMA), and the microstructure evolution of the solders with Ni doping was investigated. It was observed that Ni migrated to the board Cu-side, while Cu tended to migrate toward the Ni/Au package side, and two different types of $(Cu,Ni)_6Sn_5$ intermetallic compounds (IMCs), one with 19.8 at.% to 23.4 at.% Ni and the other with 1.3 at.% to 6.4 at.% Ni content, were found. Regarding interfacial reactions, it was identified that the local Ni and Cu concentrations affected the formation of $(Cu,Ni)_6Sn_5$. Redistribution of Ni and Cu was correlated with the formation mechanism of interfacial $(Cu,Ni)_6Sn_5$.

Key words: Pb-free solders, soldering, Ni doping, packaging, interfacial reaction

INTRODUCTION

Ni and Cu are common surface finishes used in microelectronic packages, such as under bump metallurgy (UBM), substrates, and printed circuit boards (PCBs).[1,2] In the past, Sn-Pb alloys were the appropriate materials for solder joints. Nowadays, near-eutectic Sn-Ag-Cu alloys are widely used to replace Sn-Pb alloys due to environmental concerns.[3,4] To improve solder joint reliability, many studies have attempted to add minor elements, e.g., Ni,[5–8] Zn,[7–9] Mn,[7,8] Ti,[7,8] Fe,[7,8] Co,[7,8] and rare earths,[10] to Sn-Ag-Cu solder alloys. In addition to the effects on solder fatigue properties under thermal cycling, such minor doping can affect mechanical and thermal properties, due to variable combinations of interfacial reactions between solder and surface finishes.

Ni is one of the additional alloying elements that can enhance the drop and impact resistance of solder joints.[5,6] It is reported that 0.05 wt.% Ni added to Sn-0.7Cu solder can mitigate crack formation at the IMC layers between the solder and Cu substrate.[11] In addition, a Ni concentration in Sn-2.5Ag-0.8Cu solder larger than 0.005 wt.% can effectively suppress the formation of Cu_3Sn at the interface.[12] These are due to the effects of minor additions of Ni on the interfacial reactions of Sn-Ag-Cu and Sn-Cu solders with Cu substrates. Nevertheless, when these solders reacted with Ni and Cu substrates in flip-chip applications, cross-interaction occurred. Such cross-interaction was attributed to Cu and Ni diffusion from one side to the other between the Cu and Ni substrates. Wang and Liu reported that various microstructures

(Received February 27, 2010; accepted August 16, 2010; published online September 14, 2010)

developed at both sides in the Ni/Sn/Cu sandwich structure after reflow.[13,14]

In this study, Sn-3.0Ag-0.5Cu (SAC) and Sn-3.0Ag-0.5Cu-0.1Ni (SAC-0.1Ni) were jointed with electroplated Ni/Au surface finish on ball grid array (BGA) packages and Cu pads on printed circuit boards (PCBs). The objective of this work is to understand how the concentration variation of Cu and Ni affects the microstructure and phase formation in these sandwich structures.

EXPERIMENTAL PROCEDURES

Sandwich structures (Fig. 1), i.e., Cu/solder/Au/Ni, were assembled from 15 mm × 15 mm BGA packages with electrolytic Ni/Au surface finish on 2.4-mm-thick PCBs using a normal surface-mount technology (SMT) process with SAC solder paste. The PCB surface finish was organic surface preservative (OSP) on top of the Cu substrate. The diameter of the solder balls was 600 μm, and the selected chemical composition of the solder balls on the BGA packages was Sn-3.0Ag-0.5Cu or Sn-3.0Ag-0.5Cu-0.1Ni (wt.%). The Ni concentration of SAC-0.1Ni solders was evaluated by inductively coupled plasma mass spectrometry (ICP-MS). Standard SAC305 solder paste was used during SMT to assemble the BGA on PCBs. The reflow process was carried out in nitrogen atmosphere with a typical peak temperature of 240°C for 60 s above the liquid temperature, and a cooling rate of 2°C/s. After the SMT reflow process, samples were aged in the oven at 150°C for 500 h.

Cross-sectional samples were prepared by polishing and ion-beam milling (RES-101; BAL-TEC). For observation of the microstructure and interfacial morphologies, secondary-electron (SE) and backscattered-electron (BSE) modes of scanning electron microscopy (SEM) were used. The phase composition and elemental distribution were obtained by using quantitative analysis and color mapping modes, respectively, of field-emission electron probe microanalysis (FE-EPMA, JXA-8500F; JEOL). To compare growth rates of intermetallic compounds (IMCs) at the joint interface, the average thickness was measured using image analysis software.

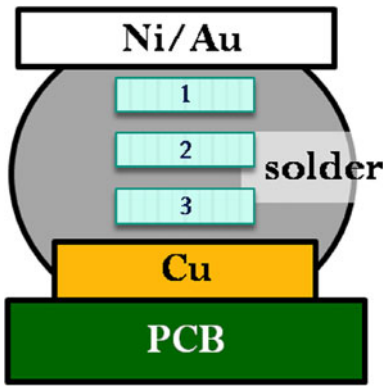

Fig. 1. Schematic diagram of the sandwich structure. Regions (1), (2), and (3) in the solder are areas selected for quantitative analysis.

RESULTS AND DISCUSSION

Microstructural Evolution and Elemental Migration in SAC and SAC-0.1Ni Solders

Figure 2 shows the microstructural variation of the SAC and SAC-0.1Ni solders between the Cu and Ni/Au substrates during aging. Inside the solder alloys, the matrix was mainly composed of eutectic regions and the β-Sn phase. In the SE images, the eutectic region with fine-lamellar Ag_3Sn and Cu-Sn phases is shown in white, while the β-Sn phase appears gray. Before aging, the eutectic phase in the SAC solders was distributed as a network structure, which was coarser than that in the SAC-0.1Ni solder. However, the eutectic region became smaller in all the solder balls after aging, and then transformed into the intermetallic compounds. From Fig. 3, a large amount of Cu_6Sn_5 and fine Ag_3Sn particles formed in the SAC solder matrix after aging. In contrast, the SAC solder doped with 0.1 wt.% Ni revealed a finer eutectic region, and tiny Cu_6Sn_5 and Ag_3Sn particles precipitated, smaller than without Ni doping.

Precipitation of the tiny Cu_6Sn_5 and Ag_3Sn particles resulted from the fact that the Ni content reduces the solubility of Cu in molten Sn.[13,14] Therefore, Cu_6Sn_5 easily nucleated due to the presence of Ni nuclei in the solder. The fine-lamellar Ag_3Sn in the eutectic region would grow along with precipitation of Cu_6Sn_5 to form particle-like Ag_3Sn, and consequently the eutectic region became finer. In addition, the Ni doping created large amounts of nucleation sites for Cu_6Sn_5. More nucleation sites resulted in retarded growth of Cu_6Sn_5. For this reason, it appears that Ni doping significantly refined the microstructure of solder alloys during heat treatment.

To investigate the variation of Cu and Ni concentration in the solders, three regions at the top (Ni/Au-side), middle, and bottom (Cu-side) of the solders were selected for investigation. For FE-EPMA, the electron beam was operated at 20 kV, and the probe size was 20 μm. Data for the three detection points were averaged in each region, and the results are presented in Table I. After reflow, the Cu concentration decreased from the Cu-side to the Ni/Au-side, while the Ni concentration decreased from the Ni/Au-side to the Cu-side. The gradients were caused by Cu and Ni dissolving from the Cu and Ni substrates, respectively. Therefore, the reflow process led to Ni dissolving into the SAC solder. As the samples were aged at 150°C for 500 h, both Cu and Ni concentrations increased at the Ni/Au- and Cu-sides, indicating that Cu migrated toward the Ni/Au-side, and Ni diffused toward the Cu-side, during aging. This cross-migration occurred in all samples, with and without Ni doping. In the literature,[7] Ni migration toward the Cu-side was

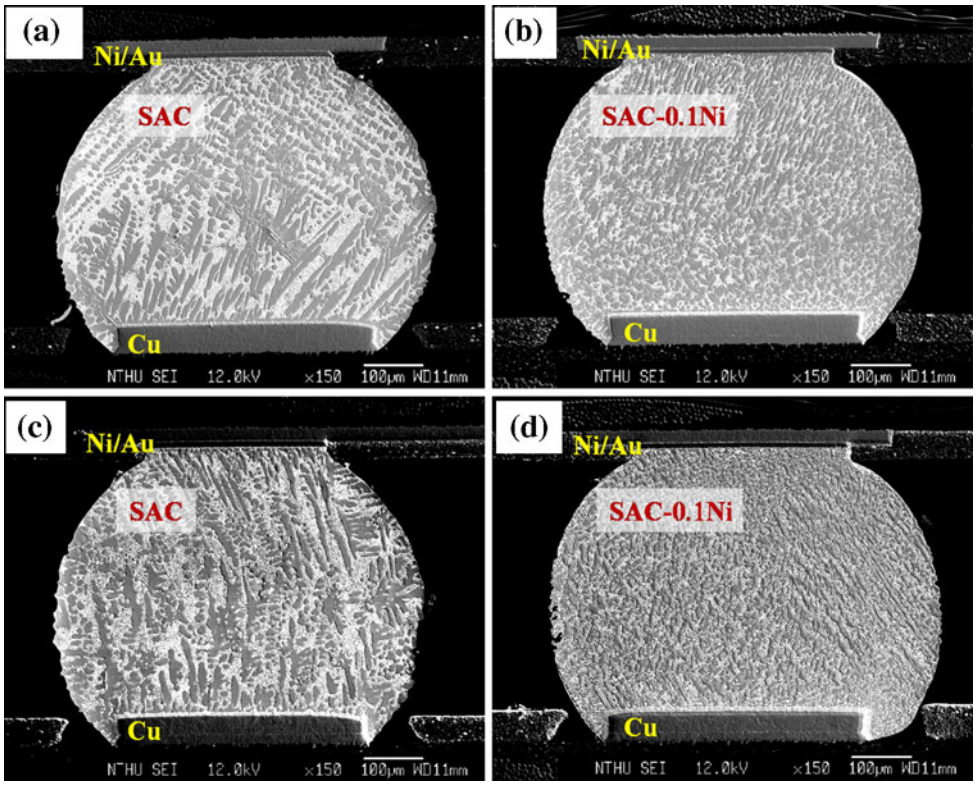

Fig. 2. SE images of the cross-sectional Ni/Au/solder/Cu structure: (a) and (b) before aging; (c) and (d) after aging at 150°C for 500 h.

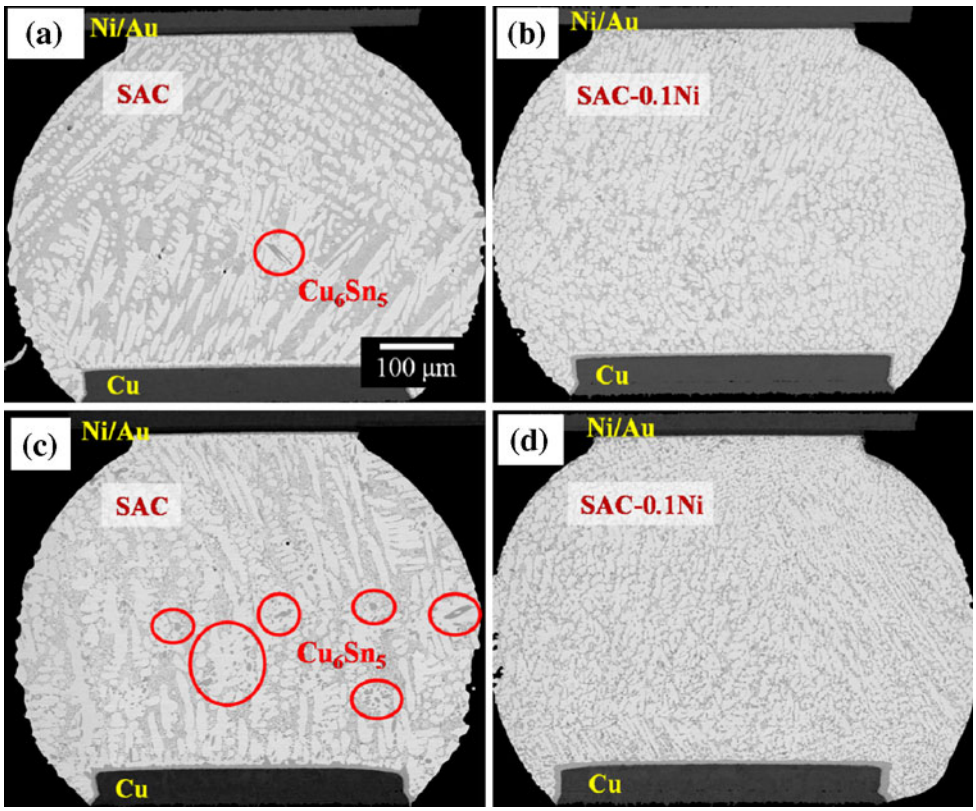

Fig. 3. BSE cross-sectional images of the Ni/Au/solder/Cu structure: (a) and (b) before aging; (c) and (d) after aging at 150°C for 500 h.

also observed in Cu/Sn-3.7Ag-0.6Cu-0.3Ni/Cu sandwich structures after aging. When Cu and Ni congregated to the Ni/Au- and Cu-sides, respectively, the formation of IMCs at both interfaces would be affected.

IMC Formation and Elemental Distribution at the Cu Side

Interfacial images between the solders and Cu pads are shown in Fig. 4. After reflow, $(Cu,Ni)_6Sn_5$ was the only IMC observed at both SAC/Cu and SAC-0.1Ni/Cu interfaces, as identified by FE-EPMA.

Table I. Cu and Ni concentration in three selected regions of the solder, as shown in Fig. 1

Assembly System	Region	Cu (wt.%)	Ni (wt.%)
As-reflowed Cu/SAC/Au/Ni	(1)	0.68 ± 0.42	0.14 ± 0.05
	(2)	0.91 ± 0.59	0.03 ± 0.02
	(3)	1.18 ± 0.07	0.02 ± 0.01
Aged Cu/SAC/Au/Ni	(1)	0.97 ± 0.15	0.16 ± 0.01
	(2)	0.72 ± 0.30	0.02 ± 0.01
	(3)	1.33 ± 0.39	0.04 ± 0.02
As-reflowed Cu/SAC-0.1Ni/Au/Ni	(1)	0.19 ± 0.08	0.17 ± 0.02
	(2)	0.43 ± 0.18	0.05 ± 0.01
	(3)	1.54 ± 0.36	0.04 ± 0.02
Aged Cu/SAC-0.1Ni/Au/Ni	(1)	0.95 ± 0.08	0.18 ± 0.02
	(2)	0.72 ± 0.50	0.01 ± 0.01
	(3)	1.22 ± 0.17	0.05 ± 0.03

However, the common phase, i.e., $(Cu,Ni)_6Sn_5$, exhibited different morphologies in these two systems. Scallop-like $(Cu,Ni)_6Sn_5$ formed at the interface of the SAC solder joint, while block-like $(Cu,Ni)_6Sn_5$ formed when Ni was doped into the system. The amount of Ni in the $(Cu,Ni)_6Sn_5$ might be the reason for the different morphologies. According to the literature,[15] $(Cu,Ni)_6Sn_5$ with a higher Ni content exhibits a faceted surface, whereas $(Cu,Ni)_6Sn_5$ with less Ni content exhibits a round surface during liquid reaction. In this study, the average Ni concentration of $(Cu,Ni)_6Sn_5$ at the interface of the Cu-side is shown in Table II. The block-like $(Cu,Ni)_6Sn_5$ at the SAC-0.1Ni/Cu interface contained more Ni than the scallop-like $(Cu,Ni)_6Sn_5$ at the SAC/Cu interface after reflow. Furthermore, the Ni concentration of the $(Cu,Ni)_6Sn_5$ adjacent to the SAC-0.1Ni solder

Table II. Average Ni concentration in the IMCs at the Cu-side

Condition	Assembly	Ni (at.%)	Phase
Before aging	SAC/Cu	2.5	$(Cu,Ni)_6Sn_5$
	SAC-0.1Ni/Cu	4.3	$(Cu,Ni)_6Sn_5$
After aging	SAC/Cu	1.3	$(Cu,Ni)_6Sn_5$
		1.0	$(Cu,Ni)_3Sn$
	SAC-0.1Ni/Cu	2.4	$(Cu,Ni)_6Sn_5$
		0.7	$(Cu,Ni)_3Sn$

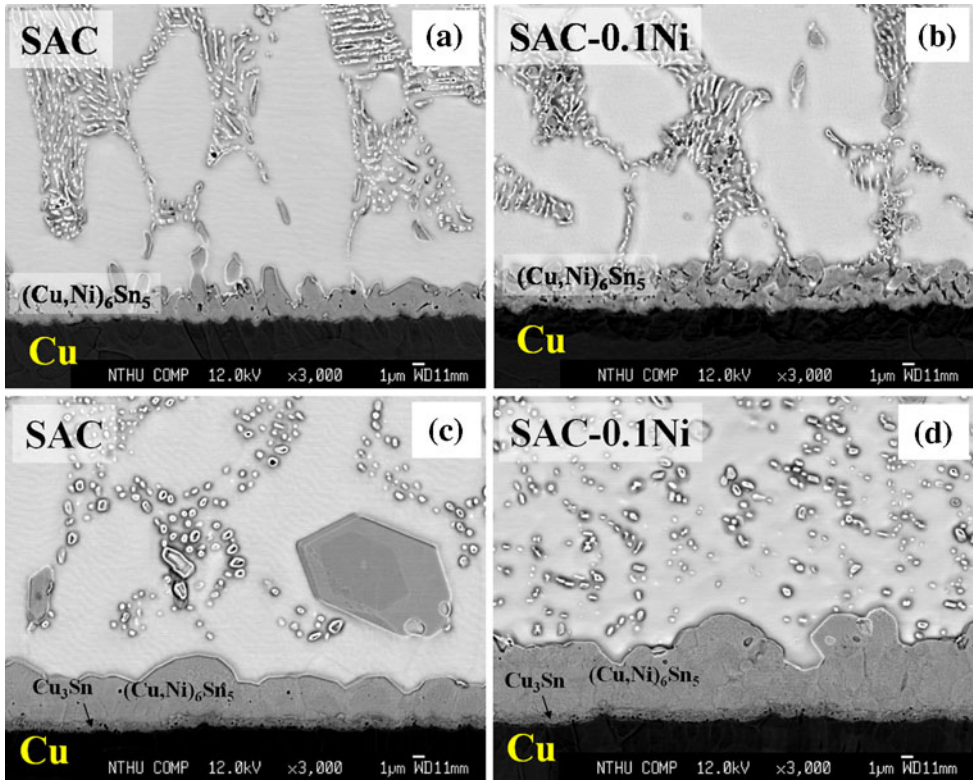

Fig. 4. BSE cross-sectional images of the interfacial IMCs at the Cu-side: (a) and (b) before aging; (c) and (d) after aging at 150°C for 500 h.

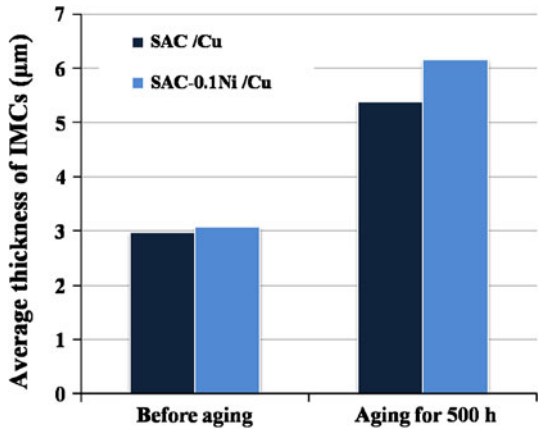

Fig. 5. Average thickness of total IMCs at the solder/Cu interfaces.

decreased slightly to that adjacent to the Cu pad at the SAC-0.1Ni/Cu interface.

The evolution of IMCs in these two assemblies on aging is shown in Fig. 4c and d. $(Cu,Ni)_6Sn_5$ became thicker and grew into a layer type in both samples. In addition to $(Cu,Ni)_6Sn_5$, thin $(Cu,Ni)_3Sn$ formed at both SAC/Cu and SAC-0.1Ni/Cu interfaces. A few Kirkendall voids were found around the thin $(Cu,Ni)_3Sn$ layer. The quantitative analysis in Table II demonstrates that the average Ni concentration in $(Cu,Ni)_6Sn_5$ decreased as new Cu_6Sn_5 grew due to the Cu flux from the substrate reacting with Sn after aging. The Ni content in $(Cu,Ni)_3Sn$ was less than that in $(Cu,Ni)_6Sn_5$, implying that Ni prefers to congregate into $(Cu,Ni)_6Sn_5$ rather than in $(Cu,Ni)_3Sn$ under this condition. The variation of IMC thickness is plotted in Fig. 5. The IMCs at the SAC-0.1Ni/Cu interface were thicker than at the SAC/Cu interface, both before and after aging, indicating that Ni addition to the SAC solder increased the growth rate of interfacial $(Cu,Ni)_6Sn_5$. Moreover, the thickness of the Cu_3Sn in the Ni-doped solder joints was similar to that in the nondoped solder joints.

The elemental distribution at the interface as revealed in Fig. 4 is represented in Fig. 6, which can be used to visualize Ni migration during aging. At the as-reflowed SAC/Cu and SAC-0.1Ni/Cu interfaces, most Ni dissolved into the interfacial $(Cu,Ni)_6Sn_5$, and the distribution was uniform. In addition to the contribution from the Ni/Au surface finish, more Ni was supplied from the solder matrix with Ni doping. Therefore, the Ni content in the $(Cu,Ni)_6Sn_5$ layer for the SAC-0.1Ni/Cu interface was larger than for the SAC/Cu interface. This is consistent with the results of quantitative analysis showing that the average Ni concentration in the $(Cu,Ni)_6Sn_5$ at the SAC-0.1Ni/Cu interface was higher than that at the SAC/Cu interface. Some Ni- and Cu-rich phases were scattered inside the eutectic region in the Ni-doped SAC solders, which were considered to be $(Cu,Ni)_6Sn_5$. This provides further evidence that Ni doping in the solder induced nucleation of $(Cu,Ni)_6Sn_5$.

After aging, the distribution of Ni in the interfacial $(Cu,Ni)_6Sn_5$ was nonuniform. A Ni-enriched region was revealed in the bottom part of the $(Cu,Ni)_6Sn_5$ layer at the SAC/Cu interface and congregated near the Cu-side. In contrast, parts of Ni-enriched region were congregated near the Cu-side, and some were scattered in the $(Cu,Ni)_6Sn_5$ at the SAC-0.1Ni/Cu interface. This difference could be correlated with the morphology of the $(Cu,Ni)_6Sn_5$ in the as-reflowed samples. It is well known that Cu at the substrate diffuses through the interfacial IMCs into the solder mainly via grain-boundary diffusion.[3] From Fig. 4b, the block-like $(Cu,Ni)_6Sn_5$ with a loose structure provides more paths for Cu diffusion out of the substrate. This is one of the reasons why $(Cu,Ni)_6Sn_5$ at the SAC-0.1Ni/Cu interface grew thicker than that at the SAC/Cu interface. During aging, new $(Cu,Ni)_6Sn_5$ with less Ni would form in the gaps between the block-like $(Cu,Ni)_6Sn_5$ grains, leading to a decrease of the average Ni concentration in the $(Cu,Ni)_6Sn_5$. Thus, the as-reflowed $(Cu,Ni)_6Sn_5$ with a higher Ni content was surrounded by new $(Cu,Ni)_6Sn_5$ with a lower Ni content.

IMC Formation and Elemental Distribution at the Ni/Au Side

At the Ni/Au-side, $(Cu,Ni)_6Sn_5$ was still the only IMC at the interface in both Ni-doped and nondoped systems. No trace of $(Ni,Cu)_3Sn_4$ was identified at the interface for samples aged after 500 h. The Cu source for the $(Cu,Ni)_6Sn_5$ was migration of Cu from the solders and dissolution of the Cu pads during reflow. In Fig. 7a and b, needle-like $(Cu,Ni)_6Sn_5$ formed at the Ni/Au/SAC and thin-layered $(Cu,Ni)_6Sn_5$ at the Ni/Au/SAC-0.1Ni interface after reflow. The aging process caused all the interfacial $(Cu,Ni)_6Sn_5$ to become layered and thick, as shown in Fig. 7c and d. The thickness of the IMCs at the Ni/Au-side was much smaller than that at the Cu-side. In contrast, thickness variations at the Cu- and Ni/Au-sides were different. The average thickness of the $(Cu,Ni)_6Sn_5$ is plotted in Fig. 8. The growth rate of $(Cu,Ni)_6Sn_5$ at the Ni/Au/SAC-0.1Ni interface was slower than that at the Ni/Au/SAC interface.

To further visualize the Ni and Cu distributions, local regions with thick IMC were selected for analysis by high-magnification color mapping, as shown in Fig. 9. It is interesting to note that there were two types of $(Cu,Ni)_6Sn_5$ formed at the as-reflowed Ni/Au/SAC interface (Fig. 9a): One, with a higher Ni content, represented as H-$(Cu,Ni)_6Sn_5$, was adjacent to the Ni/Au surface finish interface, and the other, with a lower Ni content, indicated as L-$(Cu,Ni)_6Sn_5$, was located near the interface. As presented in Table III, the quantitative analysis showed that the average Ni concentration was from

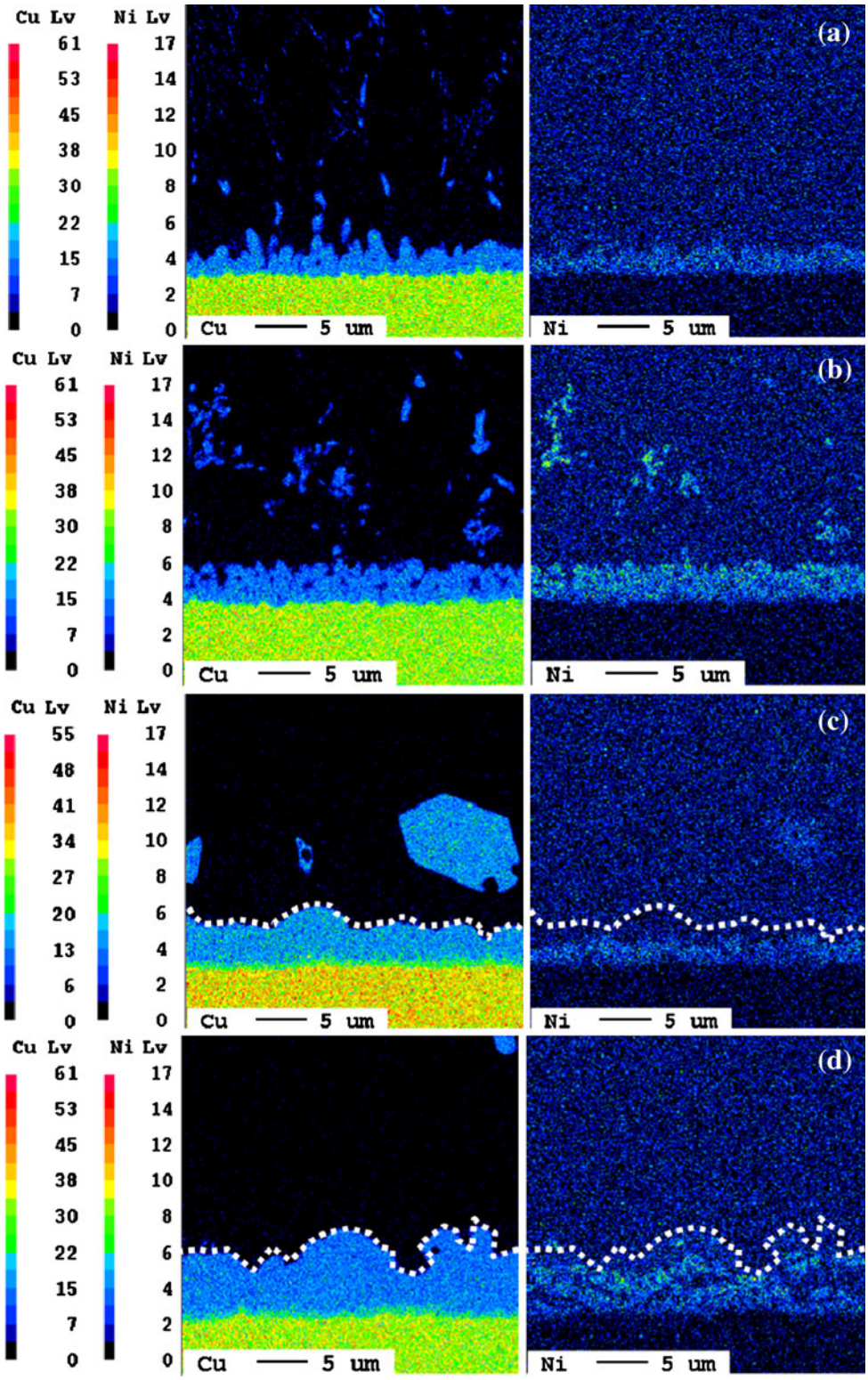

Fig. 6. Color map of the Cu and Ni distributions at the Cu-side interface, as shown in Fig. 4a–d, respectively. The *dotted line* indicates the boundary between $(Cu,Ni)_6Sn_5$ and the solder.

19.8 at.% to 23.4 at.% in H-$(Cu,Ni)_6Sn_5$, while it was from 4.7 at.% to 6.4 at.% in L-$(Cu,Ni)_6Sn_5$. Only H-$(Cu,Ni)_6Sn_5$ was found at the interface of the Ni-doped solder joint system after reflow (Fig. 9b), and the composition was similar to that in the nondoped system. This distribution was attributed

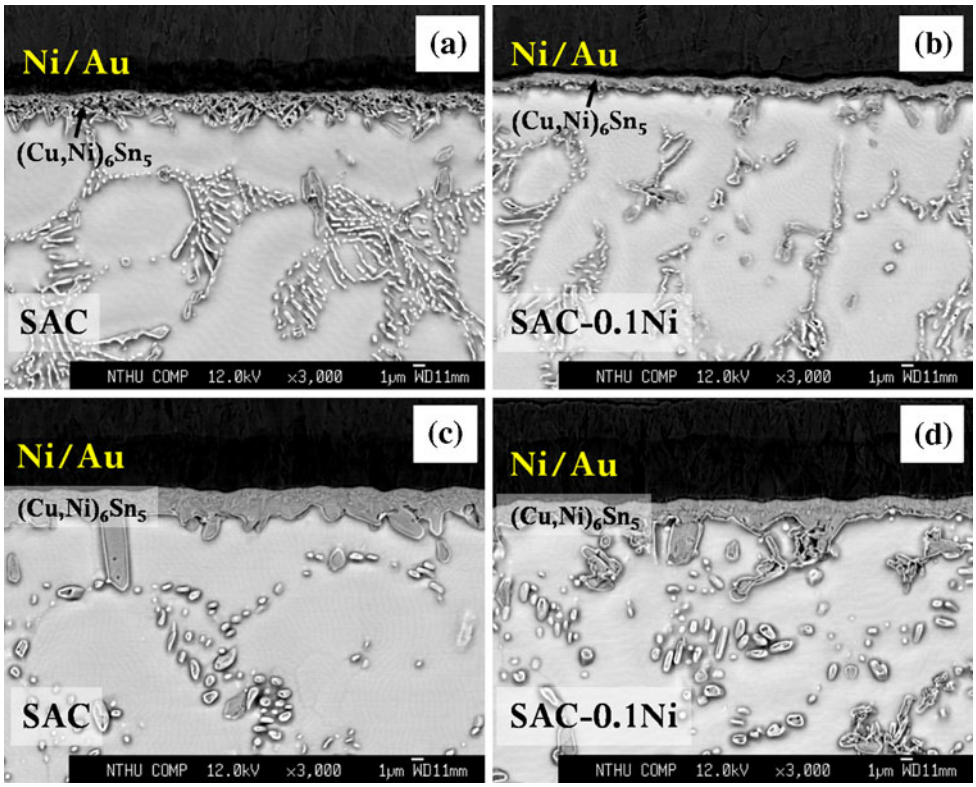

Fig. 7. BSE cross-sectional images of the interfacial IMCs at the Ni/Au-side: (a) and (b) before aging; (c) and (d) after aging at 150°C for 500 h.

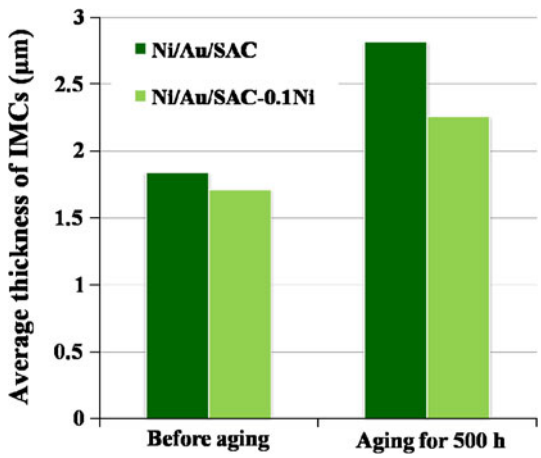

Fig. 8. Average thickness of total IMCs at the interface of Ni/Au and solders.

to the fact that the the SAC-0.1Ni solder supplied more Ni to congregate in $(Cu,Ni)_6Sn_5$ at the Ni/Au-side during reflow. Ni would not only migrate to the Cu-side, but also to the Ni/Au-side. After aging, the H-$(Cu,Ni)_6Sn_5$ grew slowly; however, the L-$(Cu,Ni)_6Sn_5$ grew significantly between H-$(Cu,Ni)_6Sn_5$ and solder in both solder joints, with and without Ni doping. In the meanwhile, the composition of H-$(Cu,Ni)_6Sn_5$ was nearly constant. In contrast, the Ni content within L-$(Cu,Ni)_6Sn_5$ at the Ni/Au/SAC interface increased slightly. The formation of L-$(Cu,Ni)_6Sn_5$ was attributed to dissolved Cu in these solders, which migrated toward the Ni/Au-side and reacted with Sn. From Table I, the Cu concentration decreased in the middle of the solders and increased near the Ni/Au-side, confirming Cu migration from the solder to the Ni/Au-side during aging.

Based on these results, the H-$(Cu,Ni)_6Sn_5$ mainly formed at the Ni/Au-side during the liquid reaction. This means that the formation of H-$(Cu,Ni)_6Sn_5$ needs enough Ni source at the high temperature. Hence, the $(Cu,Ni)_6Sn_5$ at the Cu-side is all L-$(Cu,Ni)_6Sn_5$, with 1.3 at.% to 4.3 at.% Ni. According to the literature,[3,16] Ni within the Cu_6Sn_5 can stabilize the structure, and the Gibbs free energy of $(Cu,Ni)_6Sn_5$ decreases by around 9 kJ/mol as the Ni content increases to 20 at.%. Energy and density-of-states calculations show that the compound $(Cu,Ni)_6Sn_5$ is more stable than Cu_6Sn_5, since there is a large driving force for Ni dissolution into $(Cu,Ni)_6Sn_5$, and $Cu_4Ni_2Sn_5$ is the most stable phase.[17] In this study, the composition of H-$(Cu,Ni)_6Sn_5$ is similar to that of the stable $Cu_4Ni_2Sn_5$ compound, therefore, H-$(Cu,Ni)_6Sn_5$ was considered as the most stable IMC in this system. In fact, the standard Gibbs energy of formation of Ni_3Sn_4 (−24.1 kJ/mol) is much lower than that of H-$(Cu,Ni)_6Sn_5$ (−16.0 kJ/mol).[3] The thermodynamic analysis shows that Ni_3Sn_4 possibly forms at the interface. However, no Ni_3Sn_4 was found when the Cu/SAC/Au/Ni and Cu/SAC-0.1Ni/Au/Ni systems were aged

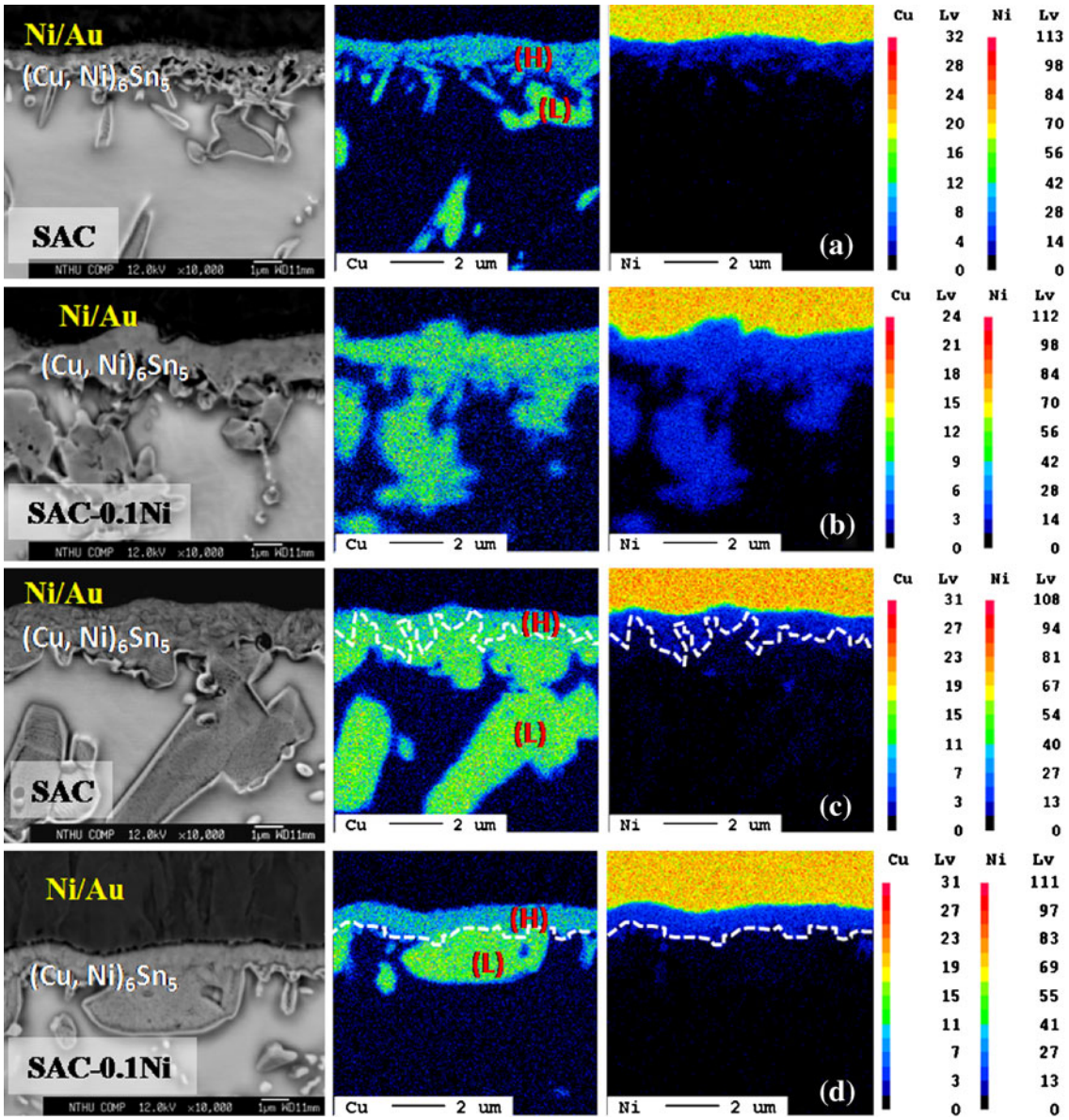

Fig. 9. Color map of the Cu and Ni distributions at the Ni/Au-side interface: (a) and (b) before aging; (c) and (d) after aging at 150°C for 500 h. The symbol (H) indicates $(Cu,Ni)_6Sn_5$ with higher Ni content, and (L) indicates $(Cu,Ni)_6Sn_5$ with lower Ni content.

Table III. Average Ni concentration in the IMCs at the Ni/Au-side

Condition	Assembly	Ni (at.%)	Phase
Before aging	SAC/Au/Ni	20.0	H-$(Cu,Ni)_6Sn_5$
		4.7	L-$(Cu,Ni)_6Sn_5$
	SAC-0.1Ni/Au/Ni	23.4	H-$(Cu,Ni)_6Sn_5$
After aging	SAC/Au/Ni	19.8	H-$(Cu,Ni)_6Sn_5$
		6.4	L-$(Cu,Ni)_6Sn_5$
	SAC-0.1Ni/Au/Ni	23.4	H-$(Cu,Ni)_6Sn_5$
		5.5	L-$(Cu,Ni)_6Sn_5$

at 150°C for 500 h. It is argued that Ni_3Sn_4 may form as more Ni diffuses into the H-$(Cu,Ni)_6Sn_5$ after long periods of aging.

CONCLUSIONS

The effects of minor Ni doping on the microstructural variations and interfacial reactions in Cu/Sn-3.0Ag-0.5Cu/Au/Ni and Cu/Sn-3.0Ag-0.5Cu-0.1Ni/Au/Ni sandwich structures were investigated. After reflow, the eutectic region in SAC solders was coarser than that in SAC-0.1Ni solder. After aging, the eutectic region became smaller. The addition of

0.1 wt.% Ni to the SAC solder joints resulted in a finer eutectic region and induced finer compound formation than without Ni doping. During aging, it was identified that Ni migrated toward the Cu-side, and Cu migrated toward the Ni/Au-side. Most Ni congregated into the $(Cu,Ni)_6Sn_5$ and affected the interfacial reactions.

Two types of $(Cu,Ni)_6Sn_5$ were detected, containing 1.3 at.% to 6.4 at.% Ni in L-$(Cu,Ni)_6Sn_5$ and 19.8 at.% to 23.4 at.% Ni in H-$(Cu,Ni)_6Sn_5$. At the Cu-side, no H-$(Cu,Ni)_6Sn_5$ was observed. Scallop-like L-$(Cu,Ni)_6Sn_5$ formed at the SAC/Cu interface, and block-like L-$(Cu,Ni)_6Sn_5$ formed at the SAC-0.1Ni/Cu interface after reflow. These different morphologies resulted in faster growth of L-$(Cu,Ni)_6Sn_5$ in the Ni-doped system than in the nondoped system during aging. In addition, the lower Ni concentration and scattered Ni distribution in L-$(Cu,Ni)_6Sn_5$ at the SAC-0.1Ni/Cu interface was related to the formation mechanism of L-$(Cu,Ni)_6Sn_5$.

At the Ni/Au-side, needle-like H-$(Cu,Ni)_6Sn_5$ and a small amount of L-$(Cu,Ni)_6Sn_5$ formed at the Ni/Au/SAC interface after reflow. However, only thin layered H-$(Cu,Ni)_6Sn_5$ was found at the Ni/Au/SAC-0.1Ni interface. After aging, H-$(Cu,Ni)_6Sn_5$ grew slowly, while L-$(Cu,Ni)_6Sn_5$ grew significantly. The phase evolution resulted from migration of Cu and Ni atoms in the solders. The growth rate of these two types of $(Cu,Ni)_6Sn_5$ in the Ni-doped system was slower than in the nondoped system. It is demonstrated in this study that minor Ni doping substantially affects the microstructural variations and interfacial reactions in these systems.

ACKNOWLEDGEMENTS

Financial support from CISCO Systems, Inc. and the National Science Council, Taiwan, under Contract No. NSC-97-2221-E-007-021-MY3 is gratefully acknowledged.

REFERENCES

1. L.F. Miller, *Proc. IEEE Electronic Components Conf.* (Piscataway, NJ: IEEE, 1968), pp. 52–55.
2. T.Y. Lee, K.N. Tu, and D.R. Frear, *J. Appl. Phys.* 90, 4502 (2001).
3. T. Laurila, V. Vuorinen, and J.K. Kivilahti, *Mater. Sci. Eng. R: Rep.* 49, 1 (2005).
4. D.R. Frear, J.W. Jang, J.K. Lin, and C. Zhang, *JOM* 53, 28 (2001).
5. F.X. Che, J.E. Luan, and X. Baraton, *Proc. 58th Electronic Components and Technology Conf.*, pp. 485–490.
6. W.H. Zhu, L. Xu, J.H.L. Pang, X.R. Zhang, E. Poh, Y.F. Sun, A.Y.S. Sun, C.K. Wang, and H.B. Tan, *Proc. 58th Electronic Components and Technology Conf.*, pp. 1667–1672.
7. I.E. Anderson and J.L. Harringa, *J. Electron. Mater.* 35, 94 (2006).
8. I.E. Anderson, *J. Mater. Sci: Mater. Electron.* 18, 55 (2007).
9. M.G. Cho, S.K. Kang, D.Y. Shih, and H.M. Lee, *J. Electron. Mater.* 36, 1501 (2007).
10. C.M.L. Wu, D.Q. Yu, C.M.T. Law, and L. Wang, *Mater. Sci. Eng. R: Rep.* 44, 1 (2004).
11. K. Nogita, C.M. Gourlay, and T. Nishimura, *JOM* 61, 45 (2009).
12. Y.W. Wang, C.C. Chang, and C.R. Kao, *J. Alloys Compd.* 478, L1 (2009).
13. S.J. Wang and C.Y. Liu, *Scripta Mater.* 55, 347 (2006).
14. S.J. Wang and C.Y. Liu, *J. Electron. Mater.* 35, 1955 (2006).
15. J.Y. Tsai, Y.C. Hu, C.M. Tsai, and C.R. Kao, *J. Electron. Mater.* 32, 1203 (2003).
16. P. Yao, P. Liu, and J. Liu, *Microelectron. Eng.* 86, 1969 (2009).
17. C. Yu, J. Liu, H. Lu, P. Li, and J. Chen, *Intermetallics* 15, 1471 (2007).